

Multi-Material Continuum Topology Optimization for Embodied Carbon Objectives

by

Claire Elizabeth Holley

B.S. Civil and Environmental Engineering
Massachusetts Institute of Technology, 2021

SUBMITTED TO THE DEPARTMENT OF CIVIL AND ENVIRONMENTAL
ENGINEERING IN PARTIAL FUFILLMENT OF THE REQUIREMENTS FOR THE
DEGREE OF

MASTER OF ENGINEERING IN CIVIL AND ENVIRONMENTAL ENGINEERING

AT THE

MASSACHUSETTS INSTITUTE OF TECHNOLOGY

June 2021

© 2021 Claire Holley. All rights reserved

The author hereby grants to MIT permission to reproduce and to distribute publicly paper and
electronic copies of this thesis document in whole or in part in any medium now known or
hereafter created.

Signature of Author
Department of Civil and Environmental
May 14, 2021

Certified by
Josephine V. Carstensen
Assistant Professor of Civil and Environmental Engineering
Thesis Supervisor

Accepted by
Colette L. Heald
Professor of Civil and Environmental Engineering
Chair, Graduate Program Committee

Multi-Material Continuum Topology Optimization for Embodied Carbon Objectives

by

Claire E. Holley

Submitted to the Department of Civil and Environmental Engineering on May 14th 2021 in Partial Fulfilment of the Requirements for the Degree of Master of Engineering in Civil and Environmental Engineering

Abstract

Recent years have seen an increase in research and practical interest that seek to lower the carbon footprint of infrastructure and building design. Typically, carbon emissions from the built environment are divided into two categories: operational emissions and embodied carbon. Over the past decades, most work has focused on lowering the operational carbon, so now attention has turned to lowering the embodied carbon, which constitutes a significant proportion of the carbon emissions over the lifecycle of a building. Within structural design of buildings and infrastructure, topology optimization is an emerging technology, often seeking to make structures more materially efficient. It therefore offers a means to reduce the structural weight, and as such, minimize the global warming potential (GWP). This research provides an exploration of bi-material optimization problems that minimize GWP as well as compliance for a series of representative models. Two materials are considered; one with a stiff, high embodied carbon coefficient (ECC) material, such as steel, and a less stiff, lower ECC material, such as timber or concrete.

This work presents multi-material topology optimization frameworks that lower the embodied carbon for continuum design. For both cases of compliance and GWP minimization, an additional set of design variables are used to control the material selection. The framework uses a density-based approach to topology optimization and existing multi-material formulations. For the design, the Solid Isotropic Material with Penalization (SIMP) method is used to penalize intermediate material choices and *fmincon* is taken as the gradient based optimizer. The frameworks are demonstrated on several benchmark examples and compared between the two optimization problems. In both cases, the stiffer material was generally placed near supports and where loading is applied. The results show not only optimization through material selection, but topology optimization in shape and size.

Keywords: Topology Optimization, Continuum, Multi-Material, Compliance, Embodied Carbon

Thesis Supervisor: Josephine V. Carstensen

Title: Assistant Professor of Civil and Environmental Engineering

Acknowledgements

I would sincerely and wholeheartedly like to thank my advisor, Professor Josephine Carstensen, for providing me with support and inspiration throughout this whole process. I would not have been able to do this without your thoughtful guidance.

And I would also like to thank my family, friends, and fellow students who not only encouraged me academically, but made life in general that much more enjoyable.

Table of Contents

Abstract	3
Acknowledgements	5
1. Introduction	7
2. Literature Review	11
3. Methodology	13
3.1 Single Material Continuum Topology Optimization	13
Problem Formulation	13
SIMP Analysis	15
Density Filter Analysis	16
3.2 Bi-Material Continuum Topology Optimization with SIMP	17
Problem Formulation	17
Results	18
3.3 Bi-Material CTO with Compliance Objective and GWP Constraint.....	20
Problem Formulation	20
Results	21
3.4 Bi-Material CTO with GWP Objective and Compliance Constraint.....	22
Problem Formulation	22
Results	23
4. Conclusions	25
5. References	26

1. Introduction

As awareness and concern of climate change has increased in recent years, the role of human activities in exacerbating global warming is being examined as a primary contributor. This paper looks specifically at the global warming potential of the carbon emissions produced by the buildings sector. Buildings sector is defined here as all of the operations involved in constructing and maintaining buildings and other infrastructure. The International Energy Agency’s Global Status Report for Buildings and Construction found that in 2018, 39% of the global energy-related carbon dioxide (CO₂) emissions were attributable to the buildings sector (IEA & UNEP, 2019). Figure 1 shows the percentages of global CO₂ emissions contributed by different market sectors, with the buildings sector partitioned into more detailed sections. The distinction between dark and lighter blue in the chart represents the distinction made between embodied and operational carbon when considering the emissions of a building over its entire lifecycle.

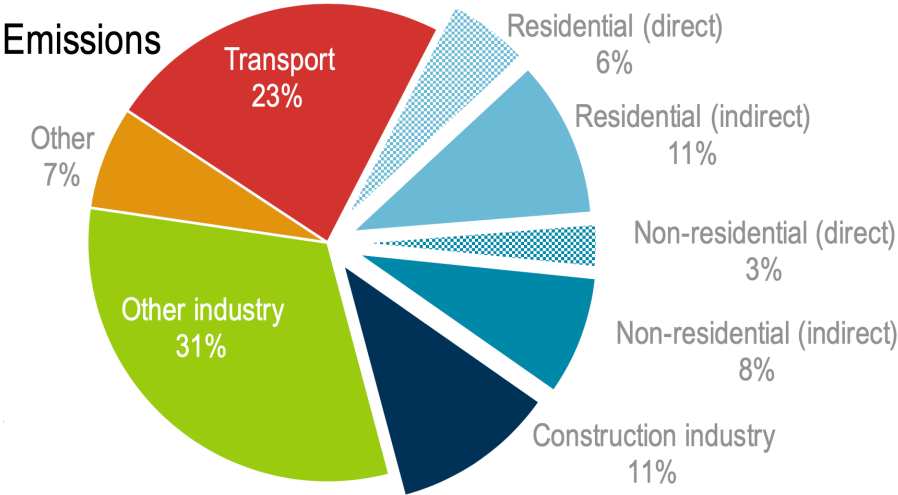


Figure 1: Global CO₂ emissions by sector; buildings sector shown in blue (IEA & UNEP, 2019)

Operational carbon is defined as “the carbon dioxide and equivalent global warming potential (GWP) of other gases associated with the in-use operation of the building. This usually includes carbon emissions associated with heating, hot water, cooling, ventilation, and lighting systems, as well as those associated with cooking, equipment, and [elevators],” (LETI, 2020). They also define **embodied carbon** as “the carbon emissions associated with the extraction and processing of materials, the energy and water consumption used by the factory in producing products, transporting materials to site, and constructing the building.” Though there are alternative

definitions for these terms that may encompass more or less factors, the definitions provided here are what will be referenced throughout the paper. In Figure 1, the light blue sections indicate the operational carbon emissions produced from residential and non-residential buildings. The section labelled “Construction industry” signifies the emissions contribution from the processes required to construct a building, or, the embodied carbon. Regarding the carbon emissions associated with a building during its lifecycle, all of the initial emissions due to construction and materials are from the embodied carbon. Then, the majority of the emissions from the remainder of its lifecycle results from the operation of the building, excepting those from any physical maintenance or upgrades to the building and from its demolition. The lifecycle of a building’s carbon emissions is exemplified in Figure 2.

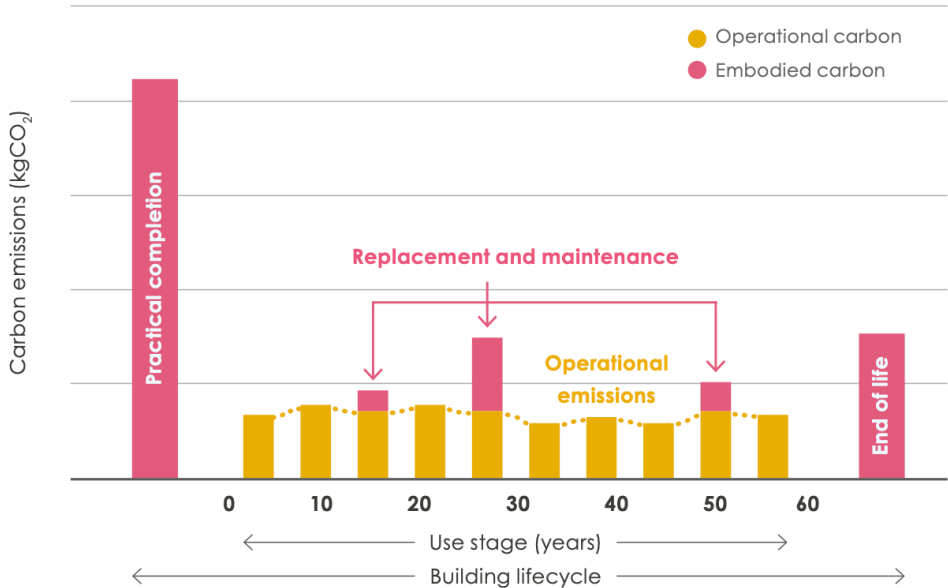


Figure 2: Lifecycle carbon emissions timeline including both operational and embodied carbon (LETI, 2020)

Referencing Figure 1 again, currently operational carbon contributes over two-thirds of the emissions of the buildings sector. However, it is expected in future projections that as electricity grids decarbonize and domestic appliances become more efficient, the operational carbon of buildings will decrease (UK GBC, 2017). With this decrease in operational carbon, the influence of embodied carbon in the total emissions output of a building will increase. Thus, reducing the embodied carbon of a building will become more important. Achieving this can come in many

forms, such as decreasing emissions during transportation or the construction process, but what much research focuses on is the reduction of material usage.

Since the embodied carbon of a building is directly proportional to the mass of material used, the most straightforward way of reducing emissions is to use less material. However, it is not this simple, as buildings are typically made out of more than one material. The metric used to compare the emissions generated by the production of different materials is the Embodied Carbon Coefficient (ECC), which is expressed in terms of kilograms of equivalent CO₂ emissions per kilogram of material (kgCO₂e/kg). These values vary extensively between common building materials; for example, a structure built entirely out of steel will have about ten times the embodied carbon as a concrete structure that has the same mass (Hammond & Jones, 2011). However, since steel is a much stronger and stiffer material, less mass is required to perform comparably to concrete (BCSA, 2003). This question of how to combine materials with the goal of reducing embodied carbon while retaining structural performance can be investigated through topology optimization, which is the subject of this study.

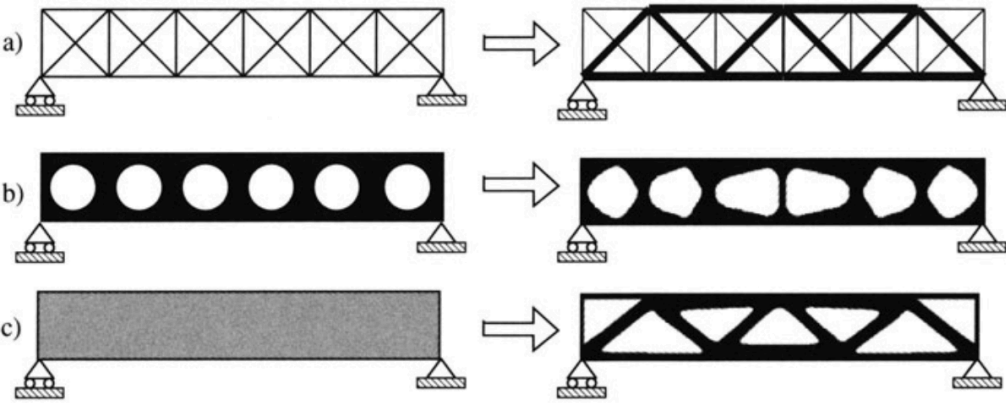


Figure 3: Illustrates the 3 main structural optimization methods - a) sizing optimization, b) shape optimization, and c) topology optimization (Bendsøe & Sigmund, 2004)

Topology optimization (TO) is a type of structural optimization in which not only are the size and location of structural features determined, but also their connectivity within a given domain, as can be seen in Figure 3 (Bendsøe & Sigmund, 2004). During this process, a mathematical evaluation method is used to determine where material is required in the design space to achieve an optimal performance value. Conventionally, the design formulation employs Finite Element Method (FEM) to evaluate a compliance minimization problem, which is the minimalization

equivalent of maximizing global stiffness. Boundary conditions, such as loading and support conditions and the dimensions of the design space, are known prior to the outset of optimization. Constraints, usually consisting at least of the structure being subject to equilibrium, can be applied to the problem construction to narrow the optimal possibilities to within their scope.

Within TO, there are two main approaches: ground structure and continuum. These terms describe the design space that TO operates within. The ground structure approach is naturally discrete and consists of a grid of nodes that are all interconnected via members. The continuum approach is treated as a solid area that must be discretized into a mesh in order to be evaluated through FEM. The design variable—the part of the setup that is altered to effect change—for the ground structure is usually the cross-sectional area of the members. For the continuum, one of the design variables must be the thickness of each mesh section, which is forced to a discrete value to not allow intermediate thicknesses and thus represents the presence or lack of material. How this is achieved will be explained in more detail later in this thesis.

2. Literature Review

While it is being recognized that the buildings sector contributes immensely to global carbon emissions, currently there exists limited research on how to incorporate designing for reduced embodied carbon in the building design phase (Häkkinen et al., 2015). Though there is no single solution, using lower-EC materials and optimizing structures to use less material have been suggested to decrease the GWP of the built environment (Pomponi & Moncaster, 2016). Two papers that investigate embodied carbon as a significant design consideration look at minimizing GWP in multi-material trusses (Stern, 2018) (Ching, 2020). Stern used parametric design tools to alter two-dimensional truss geometry and material selection of member groups, comparing the GWP required to maintain equilibrium across different material combinations. Ching also explored structural optimization of trusses with two materials, but from a topology optimization and FEM approach. Since these studies focused on trusses, they are limited to individual structural components, and cannot consider structural optimization on the scale of an entire building.

Conversely, research has been done aimed at reducing material usage within a single material continuum system. Stromberg et al. (2011) used topology optimization to conceptually design lateral resistance to wind loads for a building. Additionally, TO is often applied in practical usage to minimize or constrain by weight, such as with diaphragm arrangement in the girders of suspension bridges (Baandrup et al., 2020) and designing lightweight aircraft components (Munk et al., 2019). If the objective is minimum weight, then compliance or stress constraints are applied to the problem to ensure structural capacity beyond just static equilibrium (Bruggi & Duysinx, 2012) (Navarrina et al., 2005). With performing TO with only one material, since weight is directly proportional to volume, minimizing weight will yield the same result as minimizing volume, or even GWP. However, when optimizing with two or more materials that have different Young's moduli and densities (and ECCs), the problem becomes more complex and the tradeoffs must be considered.

Material choice can be introduced as a design variable for continuum TO through material interpolation schemes, of which several approaches have been suggested (Bendsøe & Sigmund, 1999; Yin & Ananthasuresh, 2001; Gaynor et al., 2014; Watts & Tortorelli, 2016; Sanders et al., 2018). Multi-material continuum TO has been used to evaluate minimum compliance and weight

problems (Li & Kim, 2018) and for thermomechanical buckling criteria (Wu et al., 2019), among others. However, to the author's extent of knowledge, there exists no literature examining GWP in multi-material continuum topology optimization. Using TO on multi-material systems during the conceptual design phase has a large potential to reduce GWP in the buildings sector.

3. Methodology

To explore these problems, the gradient-based optimization function *fmincon* was used in MATLAB to iterate through a 2D continuum FEM script (MathWorks, 2021). The initial setup of one of the example sections used to illustrate the TO process, the half MBB beam, is shown in Figure 4 with its loading and support conditions.



Figure 4: Initial setup of the half MBB beam. The support conditions are rollers along the left side and one at the bottom right corner. The force is applied in the negative vertical direction at the top left corner.

3.1 Single Material Continuum Topology Optimization

Problem Formulation

minimize	$f = \mathbf{F}^T \mathbf{d}$	Minimum Compliance	
	t^e		
subject to	$\mathbf{K}(t^e) \mathbf{d} = \mathbf{F}$	Static Equilibrium	(1)
	$g = \sum_{e \in \Omega} t^e v^e \leq V$	Volume Constraint	
	$t_{min} \leq t^e \leq t_{max} \quad \forall e \in \Omega$	Bounds on t^e	

Where:

- t^e is the mesh element thickness
- \mathbf{F}^T is the global force vector
- \mathbf{d} is the global displacement vector
- \mathbf{K} is the global stiffness matrix
- v^e is the mesh element area
- V is the volume constraint value

This problem formulation describes a compliance minimization problem within the continuum framework for a single material with a volume constraint. The design variables are the thickness of each mesh element, which will be altered by the optimizer with the goal of making the mesh as stiff as possible while maintaining equilibrium and without exceeding the specified volume.

As *fmincon* is a gradient-based optimizer, it uses the derivatives—also called the sensitivities or gradients—of the objective and constraint functions to guide the direction of the optimization. These sensitivities can be computed through various methods, such as finite difference and direct differentiation, but the one used for this minimum compliance problem is the adjoint method. With the adjoint method, the equilibrium constraint equation can be added to the compliance equation without changing it with the term $\lambda^T (\mathbf{K}\mathbf{d} - \mathbf{F}) = 0$. The λ term is an arbitrary, fixed vector.

The following equations show the new altered objective equation and how its sensitivity is derived:

$$\tilde{f} = \mathbf{F}^T \mathbf{d} + \lambda^T (\mathbf{K}\mathbf{d} - \mathbf{F}) \quad (2)$$

$$\frac{\partial \tilde{f}}{\partial t^e} = \mathbf{F}^T \frac{\partial \mathbf{d}}{\partial t^e} + \lambda^T \left(\frac{\partial \mathbf{K}}{\partial t^e} \mathbf{d} + \mathbf{K} \frac{\partial \mathbf{d}}{\partial t^e} \right) \quad (3)$$

$$\frac{\partial \tilde{f}}{\partial t^e} = (\mathbf{F}^T + \lambda^T \mathbf{K}) \frac{\partial \mathbf{d}}{\partial t^e} + \lambda^T \frac{\partial \mathbf{K}}{\partial t^e} \mathbf{d} \quad (4)$$

$$\text{Define } \mathbf{F}^T + \lambda^T \mathbf{K} = 0, \text{ so that } \lambda^T = -\mathbf{d} \quad (5)$$

$$\text{Therefore } \frac{\partial \tilde{f}}{\partial t^e} = \lambda^T \frac{\partial \mathbf{K}}{\partial t^e} \mathbf{d} = -\mathbf{d}^T \frac{\partial \mathbf{K}}{\partial t^e} \mathbf{d} \quad (6)$$

$$\text{Define } K_0^e = \frac{K_e}{t^e E^e} \quad (7)$$

$$\text{So that } \frac{\partial \mathbf{K}}{\partial t^e} = E^e K_0^e \quad (8)$$

Where E^e is the Young's modulus of a mesh element.

Calculating the sensitivity of the volume constraint is more straightforward and is:

$$\frac{\partial g}{\partial t^e} = v^e \quad (9)$$

For more in-depth sensitivity analysis, refer to (Christensen & Klarbring, 2009).

SIMP Analysis

Since the optimization problem works with continuous variables, this means that the design variable of mesh element thickness is allowed to have any value between the bounds of t_{\min} and t_{\max} (usually 0 and 1, respectively). In the case of using topology optimization on a two-dimensional section that is being loaded in-plane, however, the intention is to determine presence of material or lack thereof. The occurrence of intermediate thicknesses—that is, values not at the two extremes—is not practical to the application and should be designed away so that the thickness variable is forced to become discrete. In this investigation, this is done with **Solid Isotropic Material with Penalization (SIMP)**, though there are also other methods (Bendsøe, 1989). SIMP uses a nonlinear regularization model to make intermediate thicknesses inefficient for the model. The equations for determining K_e and $\frac{\partial K}{\partial t^e}$ with SIMP are:

$$K_e = ((t^e)^\eta + t_{\min}) E^e K_0^e \quad (10)$$

$$\frac{\partial K}{\partial t^e} = \eta (t^e)^{\eta-1} E^e K_0^e \quad (11)$$

Where η is a penalization parameter usually set to be 1 or 3. The effects of SIMP on an example section can be seen in Figure 6, compared to Figure 5 without it.

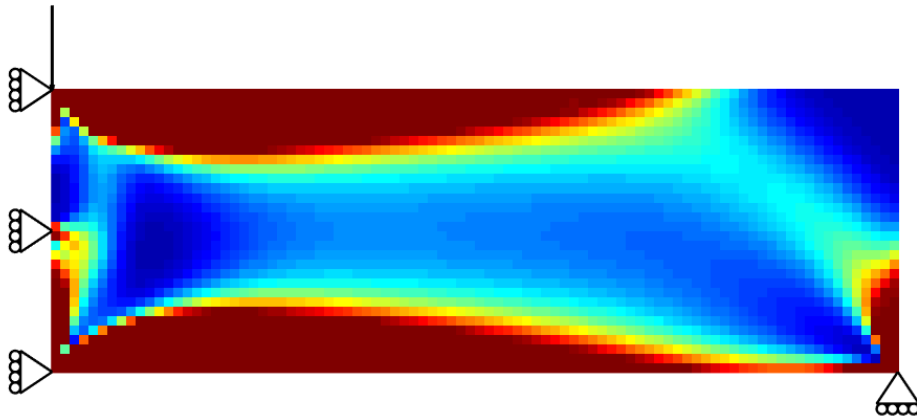


Figure 5: Continuum TO without SIMP on the half MBB example section. Fully present material is in dark red, fully voided areas in dark blue. Fictitious material is any intermediate shade.



Figure 6: Continuum TO with SIMP. Presence of material is in dark red, presence of void is in dark blue. There is little to no fictitious material.

Density Filter Analysis

Once the intermediate thicknesses have been dispelled by SIMP, there still lies another obstacle in the realization of practical topologies. As can be seen in Figure 6, a checkerboard pattern appears in the interstitial space between the broader occupied areas. This occurs because with the continuum FEM model, forces are transferred through the nodes that constitute the corners of the mesh elements, so two elements can be diagonal to each other and the model will treat them as continuous. This is not how material behaves in practice, so to simulate realism, **density filters** are applied (Bourdin, 2001) (Bruns & Tortorelli, 2001). The density filter requires that in order for an element to have material, there must be a mesh element within a specified radius (r_{\min}) that also has material.

In order to determine the distance relationships between mesh elements, a map matrix is calculated out of a standard linear weighting function. This is then multiplied with the thickness variable t^e to create a new variable t_{phys}^e to be used in the subsequent FEM analysis. The sensitivities of the objective and constraint equation also need to be multiplied by the derivative of the map function. These alterations allow the calculations to recognize more realistic physical relationships for the mesh. The difference between using density filters and not are shown by Figure 7 and Figure 6, respectively.

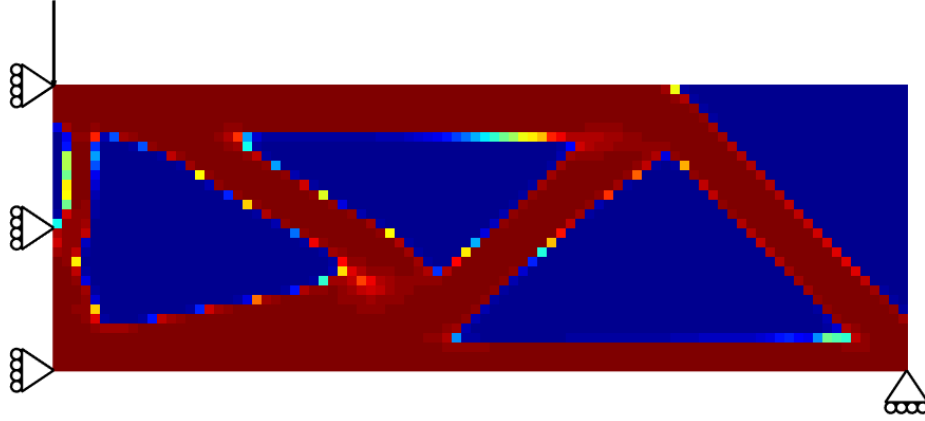


Figure 7: Continuum TO with SIMP and density filters. It no longer shows a checkerboard pattern.

3.2 Bi-Material Continuum Topology Optimization with SIMP

Problem Formulation

$$\begin{aligned}
 &\text{minimize} && f = \mathbf{F}^T \mathbf{d} && \text{Minimum Compliance} \\
 & && t^e, x^e && \\
 &\text{subject to} && \mathbf{K}(t^e, x^e) \mathbf{d} = \mathbf{F} && \text{Static Equilibrium} \\
 & && g = \sum_{e \in \Omega} t^e v^e \leq V && \text{Volume Constraint} \quad (12) \\
 & && t_{min} \leq t^e \leq t_{max} \quad \forall e \in \Omega && \text{Bounds on } t^e \\
 & && x_{min} \leq x^e \leq x_{max} \quad \forall e \in \Omega && \text{Bounds on } x^e
 \end{aligned}$$

Where:

t^e is the mesh element thickness

x^e is the material choice

The new design variable that has been introduced, x^e , controls which material is present in an individual mesh element; x_{min} represents one material, x_{max} the other. As with t^e , SIMP is used to drive x^e to a binary choice, and density filters applied to ensure that one material is not scattered within the other material. With the inclusion of two materials comes the condition that they possess different material properties. Since x^e is only used in the compliance and equilibrium equations, the only applied property that differs between materials is the Young's modulus, E^e . How it is determined which material's E^e value is used in the subsequent FEM calculations for a given mesh element is show in the equation below.

$$E(t^e, x^e) = (t^e)^\eta (E_2 + (E_1 - E_2)(x^e)^\eta) \quad (13)$$

Where E_1 and E_2 are the prespecified Young's moduli of material one and two, respectively, and η is SIMP penalization parameter. This equation, based on the inputs from t^e and x^e , results in a Young's modulus value of one of the two materials to be used in the calculation of the global stiffness matrix. Since the calculation of E now factors in both t^e and x^e , the equations for \mathbf{K} and its derivatives with respect to both variables are:

$$\mathbf{K}(t^e, x^e) = E(t^e, x^e) K_0^e \quad (14)$$

$$\frac{\partial \mathbf{K}}{\partial t^e} = \eta (t^e)^{\eta-1} (E_2 + (E_1 - E_2)(x^e)^\eta) K_0^e \quad (15)$$

$$\frac{\partial \mathbf{K}}{\partial x^e} = (t^e)^\eta (\eta (E_1 - E_2) (x^e)^{\eta-1}) K_0^e \quad (16)$$

Results

The results shown below resulted from the problem formulation described above with the choice of two materials of differing stiffnesses. The occupied volume is constrained to be half of the total volume of the design space. The three example sections consist of a cantilever, a half MBB beam, and a vertical cantilever with loading approximating gravity and wind loads.

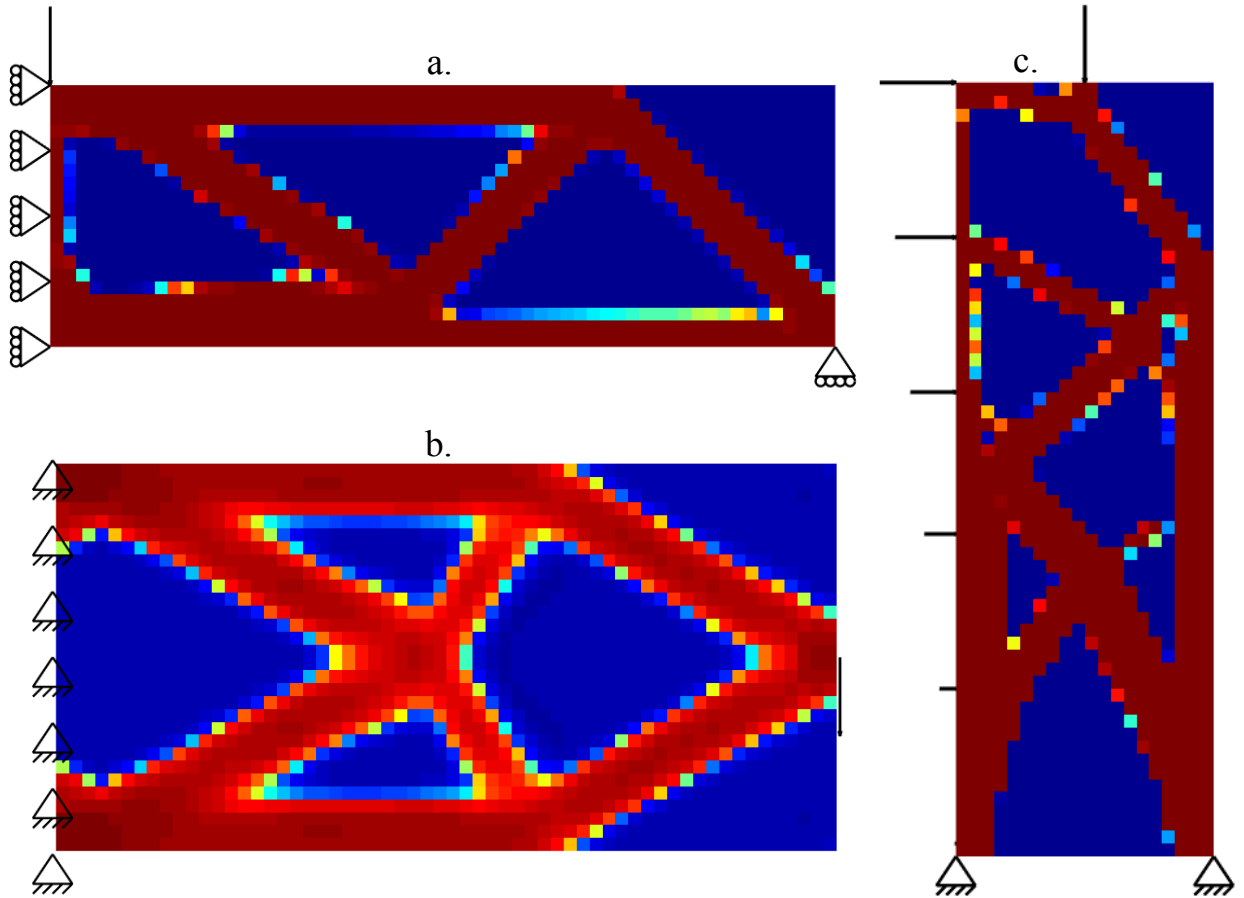


Figure 8: Multi-material CTO with minimum compliance objective and volume constraints, shown on the example sections of a. half MBB beam, b. cantilever, and c. building approximation

Though the optimization problem is designed for two materials, the results shown in Figure 8 are structures with only one material. This is because in minimizing compliance with only a constraint on the volume, the result is to assign the stiffer material to the entirety of the structure since there would be no benefit from the less stiff material. If another constraint is applied requiring that half of the resulting volume be the less stiff material, the results would be those shown in Figure 9. It is interesting to note that when limited to the amount of stiffer material able to be used, it proves most useful to be placed near the supports and at the interior of beam-type elements.

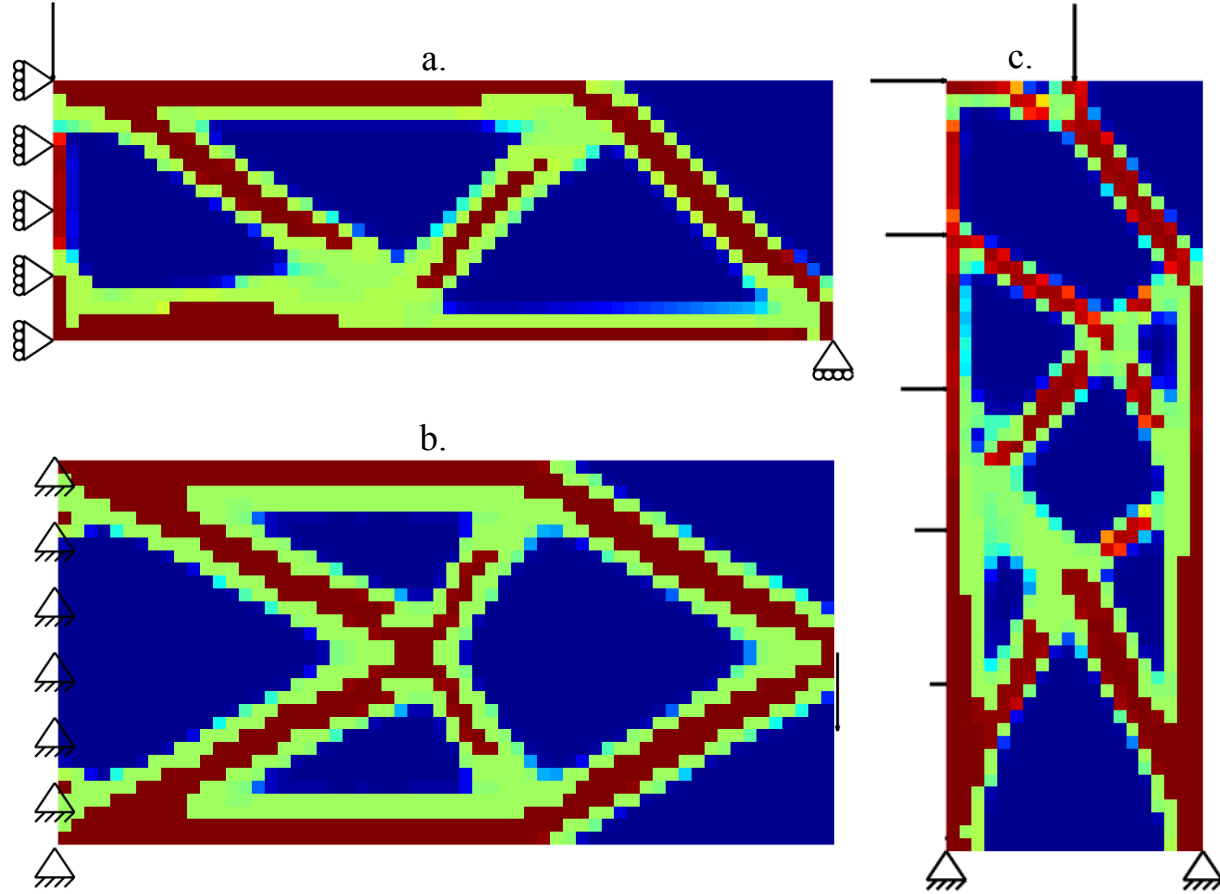


Figure 9: Multi-material CTO with minimum compliance objective and volume and material percentage constraints, shown on the example sections of a. half MBB beam, b. cantilever, and c. building approximation.

3.3 Bi-Material CTO with Compliance Objective and GWP Constraint

Problem Formulation

minimize	$f = \mathbf{F}^T \mathbf{d}$	Minimum Compliance	
t^e, x^e			
subject to	$\mathbf{K}(t^e, x^e) \mathbf{d} = \mathbf{F}$	Static Equilibrium	
	$g = \sum_{e \in \Omega} (ECC * \rho)^e v^e \leq W$	GWP Constraint	(17)
	$t_{min} \leq t^e \leq t_{max} \quad \forall e \in \Omega$	Bounds on t^e	
	$x_{min} \leq x^e \leq x_{max} \quad \forall e \in \Omega$	Bounds on x^e	

Where:

ECC^e is the material embodied carbon coefficient

ρ^e is the material density

W is the global warming potential constraint value

In this iteration of the topology optimization problem, the minimum compliance objective is conserved, however a global warming potential (GWP) constraint has replaced the volume constraint. Since the GWP constraint uses embodied carbon coefficient (ECC) and density to calculate it, this allows material choice to affect both the objective and constraint equations. The GWP calculation sums up all of the GWP values of the mesh elements with material present by multiplying the volume of each mesh element by its material density and ECC. The interpolation scheme for determining which ECC and density values to use is similar to the one used for the Young's modulus, and in this case $ECC * \rho$ is treated as one material property, as those values are always used together as a factor to directly find GWP from volume. The equation can be seen below:

$$(ECC * \rho)(t^e, x^e) = (t^e)^\eta (ECC_2 * \rho_2 + (ECC_1 * \rho_1 - ECC_2 * \rho_2)(x^e)^\eta) \quad (18)$$

Now, since the constraint equation depends on both t^e and x^e , the new sensitivities are:

$$\frac{\partial g}{\partial t^e} = \eta(t^e)^{\eta-1} (ECC_2 * \rho_2 + (ECC_1 * \rho_1 - ECC_2 * \rho_2)(x^e)^\eta) v^e \quad (19)$$

$$\frac{\partial g}{\partial x^e} = (t^e)^\eta (\eta(ECC_1 * \rho_1 - ECC_2 * \rho_2)(x^e)^{\eta-1}) v^e \quad (20)$$

Results

For the two different materials, the Young's modulus ratio was 2:1 and the $ECC * \rho$ ratio was 4:3, with material 1 having the larger values for both. The GWP constraint consists of half of the design space volume multiplied by the smaller $ECC * \rho$ value. Figure 10 displays the results in the three example sections. The three different results show varying proportions of volume that the stiff material occupies, with the cantilever being all stiff material. This could be due to the cantilever, and to a lesser extent the half MBB, requiring less volume to be stiff, and therefore being able to be under the maximum GWP constraint while allowing the stiffer, higher GWP material. The shape of the resulting cantilever and half MBB forms in this problem both closely

resemble the results in section 3.2, whereas the building approximation has an altered shape with fewer, thicker beam-type elements.

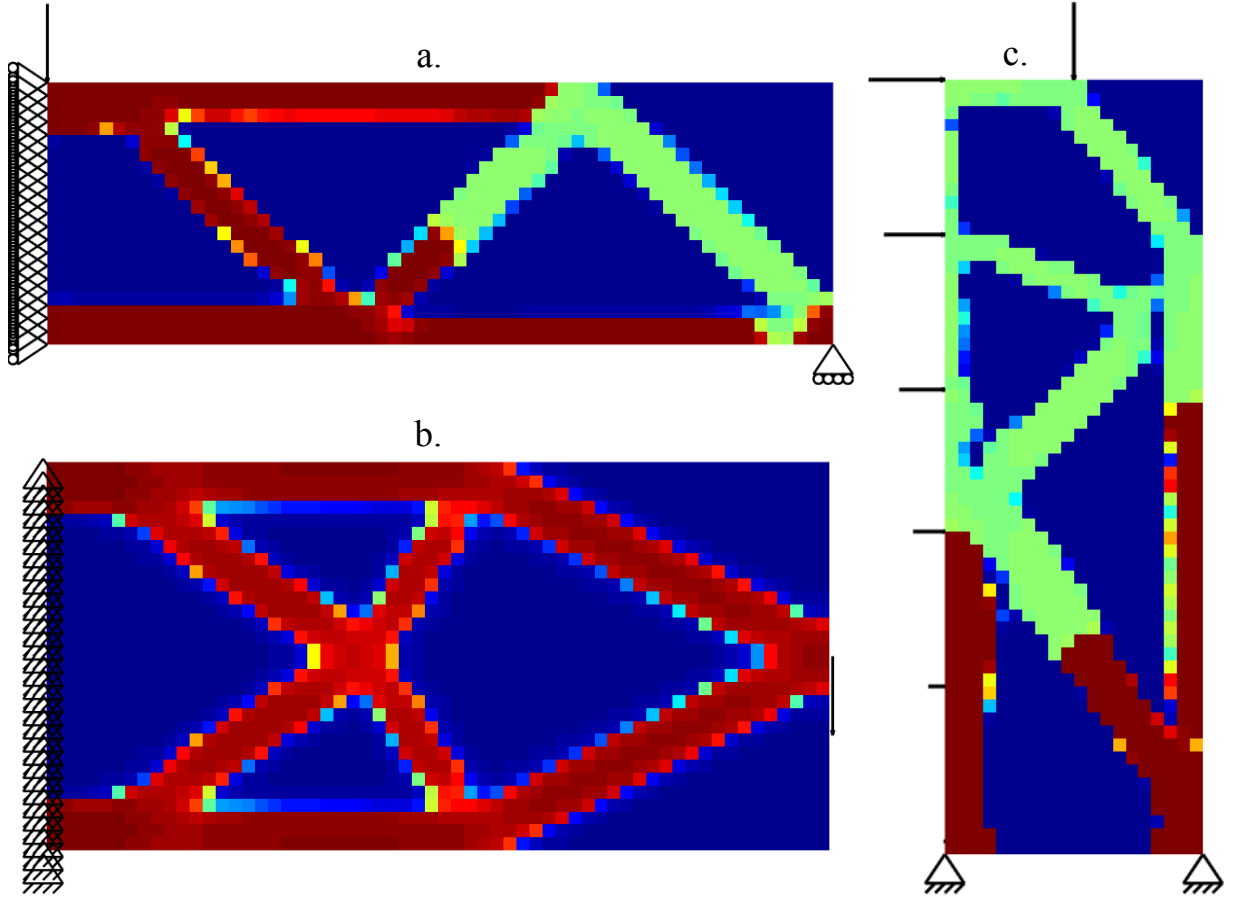


Figure 10: Multi-material CTO with minimum compliance objective and GWP constraint, shown on the example sections of a. half MBB beam, b. cantilever, and c. building approximation.

3.4 Bi-Material CTO with GWP Objective and Compliance Constraint

Problem Formulation

minimize	$f = \sum_{e \in \Omega} (ECC * \rho)^e v^e$	Minimum GWP	
t^e, x^e			
subject to	$\mathbf{K}(t^e, x^e) \mathbf{d} = \mathbf{F}$	Static Equilibrium	
	$g = \mathbf{F}^T \mathbf{d} \leq C$	Compliance Constraint	(21)
	$t_{min} \leq t^e \leq t_{max} \quad \forall e \in \Omega$	Bounds on t^e	
	$x_{min} \leq x^e \leq x_{max} \quad \forall e \in \Omega$	Bounds on x^e	

Where:

C is the compliance constraint value

For this problem formulation, the objective and constraint equations have been interchanged from the previous one, so that now the optimization is working towards minimum GWP. Similar to before, if there were no other constraints other than static equilibrium, the result would be entirely populated by the less stiff, lower GWP material. Consequently, the structure is constrained by a maximum compliance value that it must be below. Since the two equations were exchanged but remain functionally unchanged, it follows that their sensitivities will also be the same as before.

Results

The Young's moduli and GWP values used for the two materials are the same as described in the minimum compliance problem in section 3.3. The compliance constraint C was obtained by taking the value achieved in the compliance minimization problem for each example section and adding two percent. The resulting structures are shown in Figure 11. Comparing to the results from section 3.3, the building approximation has the most similar shape, with the most notable difference being a lower proportion of stiff material. The half MBB also has a relatively similar form to its previous result, however the rightmost diagonal is longer, showing that with the new objective, not only does the ratio of the amount of the two materials change, but also the shape of the structure. This latter outcome is most evident in the cantilever, which still only consists of the stiffer, higher GWP material even when the objective is to minimize GWP. The reduction in volume—and consequently GWP—comes from the change into a simpler shape of just two members connecting the supported corners to the location of the applied force.

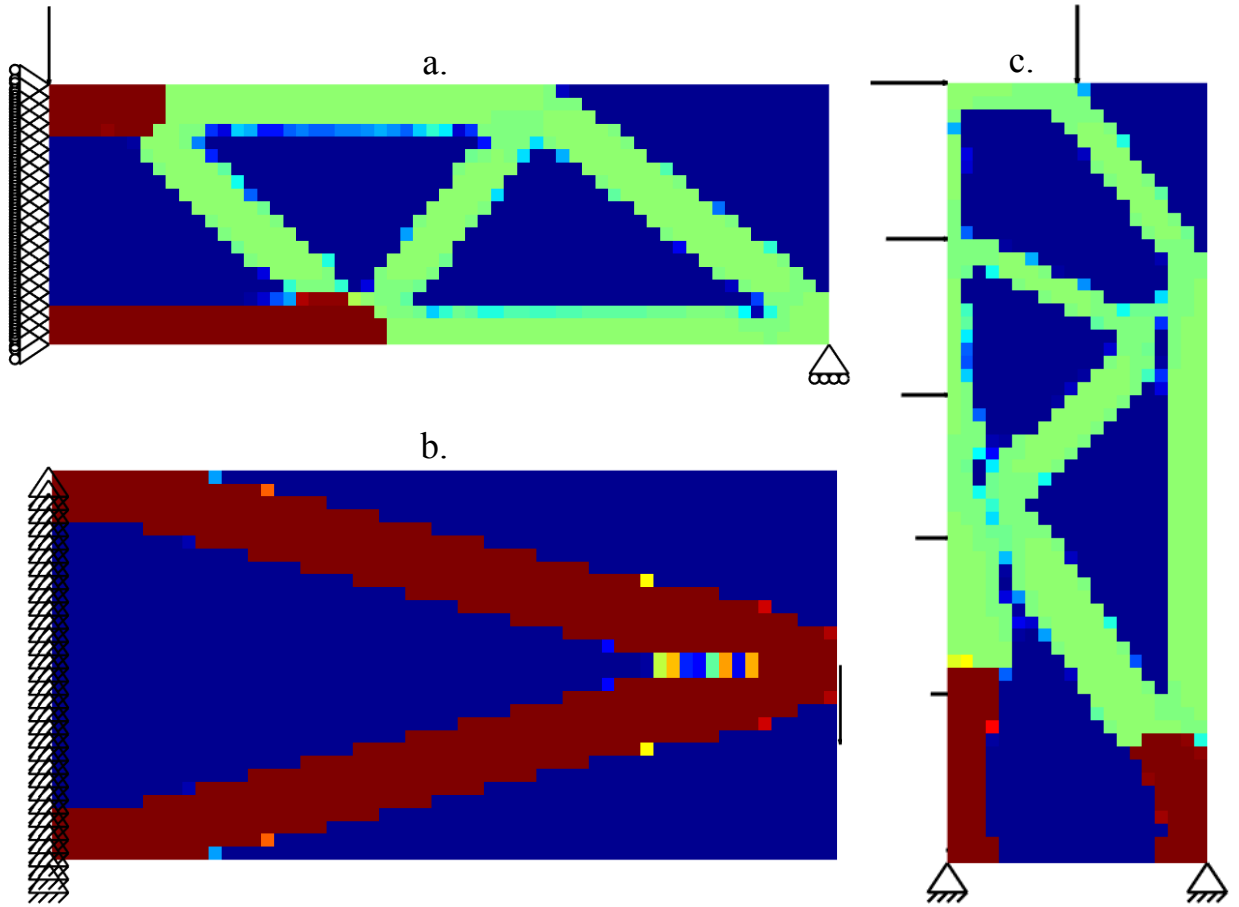


Figure 11: Multi-material CTO with minimum GWP objective and compliance constraint, shown on the example sections of a. half MBB beam, b. cantilever, and c. building approximation.

4. Conclusions

The results of the bi-material optimization problems show an interesting contrast in how the two materials are distributed throughout the resulting topology. When minimizing compliance, since one material is twice the stiffness of the other, the optimization clearly favored using that material in a smaller volume over more volume of the less stiff material. Similar to the minimization of GWP, the stiffer material was placed near the supports and along the bottom of the structures. This shows that stiffness is valued more in those locations for the overall structure. The results of the cantilever section demonstrate the capacity of TO to optimize material selection, member size, and shape since to minimize GWP, the result was fully the stiffer, higher GWP material. Though this thesis is by no means a complete investigation into the full extent of multi-material continuum topology optimization, the intention to explore the potential of using it as a tool for conceptual design was realized.

This study endeavored to establish a framework for using continuum TO with multiple materials, so naturally there are some considerations that lie outside the scope of what was done. Due to the nature of the compliance minimization problem, the structural capacity of the design is only evaluated through stiffness without taking strength or buckling into account. As mentioned previously, other studies have addressed this by including stress and/or buckling constraints, which was not covered here. Regarding the mechanics of the modelled materials, the FEM used assumes all materials are linear elastic and isotropic, where, in reality, there are common building materials that are anisotropic, such as timber.

In further studies with multiple materials, case studies using the mechanical properties of real materials would be done to investigate the effects of their interactions on GWP. Additionally, performing multi-objective optimization with both compliance and GWP as objectives would be interesting as the equations work against each other.

5. References

- Baandrup, M., Sigmund, O., Polk, H., & Aage, N. (2020). Closing the gap towards super-long suspension bridges using computational morphogenesis. *Nature Communications*, *11*(1), 2735. <https://doi.org/10.1038/s41467-020-16599-6>
- Bendsøe, M. P. (1989). Optimal shape design as a material distribution problem. *Structural Optimization*, *1*(4), 193–202. <https://doi.org/10.1007/BF01650949>
- Bendsøe, M. P., & Sigmund, O. (1999). Material interpolation schemes in topology optimization. *Archive of Applied Mechanics (Ingenieur Archiv)*, *69*(9–10), 635–654. <https://doi.org/10.1007/s004190050248>
- Bendsøe, M., & Sigmund, O. (2004). Topology optimization by distribution of isotropic material. In M. Bendsøe & O. Sigmund, *Topology Optimization* (pp. 1–69). Springer Berlin Heidelberg. https://doi.org/10.1007/978-3-662-05086-6_1
- Bourdin, B. (2001). Filters in topology optimization. *International Journal for Numerical Methods in Engineering*, *50*(9), 2143–2158. <https://doi.org/10.1002/nme.116>
- British Constructional Steelwork Association. (2003). *Steel buildings*. British Constructional Steelwork Association.
- Bruggi, M., & Duysinx, P. (2012). Topology optimization for minimum weight with compliance and stress constraints. *Structural and Multidisciplinary Optimization*, *46*(3), 369–384. <https://doi.org/10.1007/s00158-012-0759-7>
- Bruns, T. E., & Tortorelli, D. A. (2001). Topology optimization of non-linear elastic structures and compliant mechanisms. *Computer Methods in Applied Mechanics and Engineering*, *190*(26–27), 3443–3459. [https://doi.org/10.1016/S0045-7825\(00\)00278-4](https://doi.org/10.1016/S0045-7825(00)00278-4)
- Ching, H. Y. E. (2020). *Truss Topology Optimization of Steel-Timber Structures for Embodied Carbon Objectives* [Master's thesis, Massachusetts Institute of Technology]. DSpace@MIT. <https://hdl.handle.net/1721.1/127282>
- Christensen, P. W., & Klarbring, A. (2009). *An Introduction to Structural Optimization*. Springer.
- Gaynor, A. T., Meisel, N. A., Williams, C. B., & Guest, J. K. (2014). Multiple-Material Topology Optimization of Compliant Mechanisms Created Via PolyJet Three-Dimensional Printing. *Journal of Manufacturing Science and Engineering*, *136*(6), 061015. <https://doi.org/10.1115/1.4028439>

- Global Alliance for Buildings and Construction, International Energy Agency and the United Nations Environment Programme. (2019). *2019 Global Status Report for Buildings and Construction*.
<https://www.worldgbc.org/sites/default/files/2019%20Global%20Status%20Report%20for%20Buildings%20and%20Construction.pdf>
- Häkkinen, T., Kuittinen, M., Ruuska, A., & Jung, N. (2015). Reducing embodied carbon during the design process of buildings. *Journal of Building Engineering*, 4, 1–13.
<https://doi.org/10.1016/j.jobe.2015.06.005>
- Hammond, G., & Jones, C. (2011). *Embodied carbon: The Inventory of Carbon and Energy (ICE)*. Building Services Research and Information Association and University of Bath.
- Li, D., & Kim, I. Y. (2018). Multi-material topology optimization for practical lightweight design. *Structural and Multidisciplinary Optimization*, 58(3), 1081–1094.
<https://doi.org/10.1007/s00158-018-1953-z>
- London Energy Transformation Initiative. (2020). *LETI Climate Emergency Design Guide*.
<https://www.leti.london/cedg>
- MathWorks. (2021). *MATLAB Documentation (Version R2021a)* [Computer software].
<https://www.mathworks.com/help/optim/ug/fmincon.html>
- Munk, D. J., Auld, D. J., Steven, G. P., & Vio, G. A. (2019). On the benefits of applying topology optimization to structural design of aircraft components. *Structural and Multidisciplinary Optimization*, 60(3), 1245–1266. <https://doi.org/10.1007/s00158-019-02250-6>
- Navarrina, F., Muiños, I., Colominas, I., & Casteleiro, M. (2005). Topology optimization of structures: A minimum weight approach with stress constraints. *Advances in Engineering Software*, 36(9), 599–606. <https://doi.org/10.1016/j.advengsoft.2005.03.005>
- Pomponi, F., & Moncaster, A. (2016). *Embodied carbon mitigation and reduction in the built environment—What does the evidence say?* <https://doi.org/10.17863/CAM.5991>
- Sanders, E. D., Aguiló, M. A., & Paulino, G. H. (2018). Multi-material continuum topology optimization with arbitrary volume and mass constraints. *Computer Methods in Applied Mechanics and Engineering*, 340, 798–823. <https://doi.org/10.1016/j.cma.2018.01.032>
- Stern, B. (2018). *Minimizing Embodied Carbon in Multi-Material Structural Optimization of Planar Trusses* [Master's thesis, Massachusetts Institute of Technology]. DSpace@MIT.
<http://hdl.handle.net/1721.1/119324>

- Stromberg, L. L., Beghini, A., Baker, W. F., & Paulino, G. H. (2011). Application of layout and topology optimization using pattern gradation for the conceptual design of buildings. *Structural and Multidisciplinary Optimization*, 43(2), 165–180. <https://doi.org/10.1007/s00158-010-0563-1>
- UK Green Building Council. (2017). *Embodied Carbon: Developing a Client Brief*. <https://www.ukgbc.org/sites/default/files/UK-GBC%20EC%20Developing%20Client%20Brief.pdf>
- Watts, S., & Tortorelli, D. A. (2016). An n-material thresholding method for improving integerness of solutions in topology optimization. *International Journal for Numerical Methods in Engineering*, 108(12), 1498–1524. <https://doi.org/10.1002/nme.5265>
- Wu, C., Fang, J., & Li, Q. (2019). Multi-material topology optimization for thermal buckling criteria. *Computer Methods in Applied Mechanics and Engineering*, 346, 1136–1155. <https://doi.org/10.1016/j.cma.2018.08.015>
- Yin, L., & Ananthasuresh, G. K. (2001). Topology optimization of compliant mechanisms with multiple materials using a peak function material interpolation scheme. *Structural and Multidisciplinary Optimization*, 23(1), 49–62. <https://doi.org/10.1007/s00158-001-0165-z>